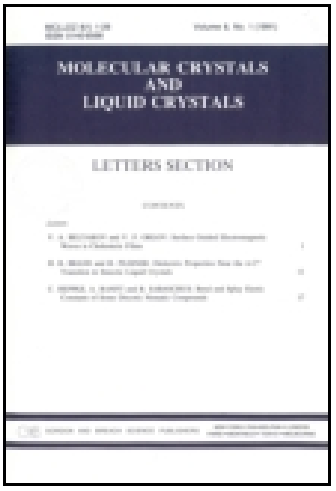

Molecular Crystals and Liquid Crystals
Publication details, including instructions for authors and subscription information:
http://www.tandfonline.com/loi/gmcl20

New Mesogenic Compounds Containing a Terminal-Substituted Benzoxazole Unit

Pei Chen[a], Yiwei Xu[a], Weisong Du[b], Guangping Zhang[b], Xinbing Chen[a] & Zhongwei An[ac]

[a] Key Laboratory of Applied Surface and Colloid Chemistry (MOE), School of Materials Science and Engineering, Shaanxi Normal University, Xi'an, P. R. China

[b] Xi'an Caijing Opto-Electrical Science & Technology Co. Ltd., Xi'an, P. R. China

[c] Xi'an Modern Chemistry Research Institute, Xi'an, P. R. China

Published online: 28 Apr 2014.

To cite this article: Pei Chen, Yiwei Xu, Weisong Du, Guangping Zhang, Xinbing Chen & Zhongwei An (2014) New Mesogenic Compounds Containing a Terminal-Substituted Benzoxazole Unit, Molecular Crystals and Liquid Crystals, 592:1, 44-62, DOI: 10.1080/15421406.2013.837997

To link to this article: http://dx.doi.org/10.1080/15421406.2013.837997

Mol. Cryst. Liq. Cryst., Vol. 592: pp. 44–62, 2014

ISSN: 1542-1406 print/1563-5287 online
DOI: 10.1080/15421406.2013.837997

New Mesogenic Compounds Containing a Terminal-Substituted Benzoxazole Unit

PEI CHEN,[1] YIWEI XU,[1] WEISONG DU,[2] GUANGPING ZHANG,[2] XINBING CHEN,[1,*] AND ZHONGWEI AN[1,3]

[1]Key Laboratory of Applied Surface and Colloid Chemistry (MOE), School of Materials Science and Engineering, Shaanxi Normal University, Xi'an, P. R. China
[2]Xi'an Caijing Opto-Electrical Science & Technology Co. Ltd., Xi'an, P. R. China
[3]Xi'an Modern Chemistry Research Institute, Xi'an, P. R. China

*A series of novel mesogenic 2-(4-alkoxyphenyl-1-yl)-benzoxazole derivatives bearing different substituents (H, NO_2, CH_3, Cl, coded as **nPB-H**, **nPB-N**, **nPB-M**, and **nPB-C**, respectively) at the 5-position were prepared and characterized. **nPB-N**, **nPB-M**, and **nPB-C** exhibited enantiotropic smectic mesophases with the mesophase ranges 3 °C–32 °C and 3 °C–82 °C on heating and cooling processes, whereas **nPB-H** showed no mesophases. The substituents with the stronger electron withdrawing effect let to the wider mesomorphic temperature domain. The **nPB-M**, **nPB-C**, and **nPB-H** displayed intense emission in CH_2Cl_2 solutions with λ_{max} peaks of the photoluminescence spectra at 350–355 nm when excited at their absorption maxima.*

Keywords Benzoxazole derivative; mesomorphic property; photophysical property

1. Introduction

Heterocyclic rings used as central cores generate numerous novel compounds that exhibit mesophases, which is attributed to their electronic unsaturation and/or their significant polarizability [1]. Among them, five- and six-membered rings have been most studied, due to their wide range of structural templates as well as their optical and photochemical properties, such as benzothiazoles [2], flavones and isoflavones [3,4], coumarins [5–7], benzothiadiazoles [8,9], and benzoxazoles [10,11]. The field involving the design and synthesis of mesogenic heterocyclic compounds has emerged as an area of active research, since such materials are attractive from both a fundamental research and practical application point of view.

For benzoxazole-based mesogenic and metallomesogenic materials, there are a few reports [10–13]. The formation of mesophases for benzoxale-based compounds was found to

*Address correspondence to Xinbing Chen, Key Laboratory of Applied Surface and Colloid Chemistry (MOE), School of Materials Science and Engineering, Shaanxi Normal University, Xi'an 710062, P. R. China. Tel.: +86-29-81530719; Fax: +86-29-85310230. E-mail: chenxinbing@snnu.edu.cn

be greatly affected by polar substituents and on intramolecular and/or intermolecular forces [14,15]. There are very few reports on liquid crystals containing a terminal-substituted benzoxazole group, and recently, we studied a series of mesogenic 2-arylbenzoxazole derivatives with different polar substituents at the 5-position of terminal benzoxazole unit, where biphenyl and benzoxazole units are used as mesogenic core [16]. It is commonly accepted that molecular order in liquid crystal phases depends largely on the mesogenic core structure: its geometry, polarizability, molecular conformation, and length-to-breath ratio as well as the number and position of permanent dipole moments in the core. For this reason, altering the core structure has been regarded as one of the factors that bring significant changes to mesomorphic properties [17]. Here, a series of novel mesogenic compounds, 2-(4-alkoxyphenyl-1-yl)-benzoxazole derivatives (**nPB-x**), with a short mesogenic core composed of benzene and benzoxazole-terminated unit bearing different substituents (H, NO_2, CH_3, Cl, coded as **nPB-H**, **nPB-N**, **nPB-M**, and **nPB-C**, respectively) at the 5-position, was designed and synthesized. The structure–property relationships of the novel benzoxazole-based liquid crystals were investigated.

2. Results and Discussion

2.1 Synthesis and Characterization

A synthetic route toward **nPB-x** is illustrated in Scheme 1, where nucleophilic substitution, nucleophilic addition of 2-aminophenols with benzaldehydes, and subsequent intramolecular cyclization were carried out in turn. As a result, the objective compounds **nPB-x** bearing carbon atoms of alkoxy chain from 3 to 18 and containing polar substituents at benzoxazole unit were obtained with purities higher than 98% (high performance liquid chromatography (HPLC) or gas chromatography (GC)) and overall yields of 47%–59%. In our case, condensation of *ortho*-aminophenols and aldehydes under oxidative conditions was adopted to construct 2-substituted benzoxazole skeletons, where 2,3-dichloro-5,6-dicyanobenzoquinone (DDQ) was chosen as an oxidative reagent with a good result.

The structures of the products and intermediates were characterized by IR, ^{1}H-NMR, GC/electron ionization-mass spectrometry (EI-MS), and elemental analysis. From the IR data of compound **14PB-C**, the peaks at 1596, 1524, and 1471 cm^{-1} were attributed to the vibrations of aromatic ring skeleton. It was noted that the absorption band of C = N in the

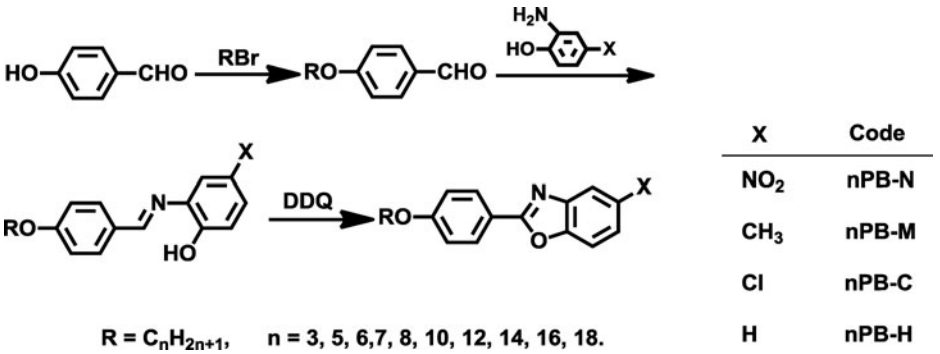

Scheme 1. Synthesis of nPB-x (nPB-N, nPB-H, nPB-M, and nPB-C series).

benzoxazole moiety was observed obviously with a blueshift to 1618 cm^{-1}. Three peaks appeared at 7.72, 7.48, and 7.30 ppm in ^{1}H-NMR spectrum of **14PB-C** were assigned to the protons of phenyl ring in 5-chlorobenzoxazole group. Two kinds of protons appeared at 8.19 and 7.03 ppm were attributed to the protons of phenyl ring. The proton in CH_2 group adjacent to oxygen atom was assigned at 4.06 ppm, and other protons in alkoxyl group appeared at 0.80–2.00 ppm. The peak of the positively charged molecular ion appeared at *m/z* 441.32 with relative intensity of 9% in GC/EI-MS spectrum for **14PB-C**, which was consistent with the theoretical one (441.24). Elemental analysis result of **14PB-C** (C 74.15, H 8.23, and N 3.22) was in accordance with the calculated data (C 73.36, H 8.21, and N 3.17). All of these results provide clear evidence that **nPB-x** series are consistent with the proposed structures.

2.2 Mesomorphic Properties

Mesomorphic properties of **nPB-x** were determined by differential scanning calorimetry (DSC) and polarizing optical microscopy (POM). DSC curves obtained under the same condition overlapped with each other, indicating that the reproducibility of the measurements was satisfactory. The phase transition temperatures reported in this paper are the peak values of the transition on DSC curves. Phase identification was made by comparing the observed textures with those reported in the literature. The phase transition temperatures, the associate enthalpy changes, and mesophase textures of **nPB-N** and **nPB-M** series are summarized in Tables 1 and 2, respectively. Clear-cut transition temperatures and textures could be obtained from DSC curves and POM observations, and they were in good agreement with each other for the multiple heating/cooling cycles. Because sliver-coated cell was obviously corrupted after DSC measurement of the samples **nPB-C**, the phase transition temperatures and mesophase textures were only determined via POM.

nPB-N, **nPB-M**, and **nPB-C** exhibited enantiotropic smectic mesophases, where the mesophase ranges were 11 °C–31 °C and 20 °C–49 °C on heating and cooling processes for compounds **nPB-N**, 3 °C–18 °C and 3 °C–37 °C for compounds **nPB-M**, and

Table 1. Types of phase transitions, temperatures, and corresponding enthalpies obtained by POM and DSC methods for compounds **nPB-N**

	Transition temperature/°C (enthalpy change/kJ mol^{-1})	
Compounds	Heating process	Cooling process
6PB-N	Cr 99.0–100.2 (n.d.) I	I 98.7–97.3 Cr
7PB-N	Cr 90.9 (17.1) SmC 100.2 (1.8) N 101.7 (0.2) I	I 98.4 (−0.2) N 97.3 (1.6) SmC 78.3(−16.3) Cr
8PB-N	Cr 92.8 (18.5) SmC 106.0 (1.9) I	I 103.2 (−1.7) SmC 75.5 (−17.8) Cr
10PB-N	Cr 82.1 (22.1) SmC 110.1 (2.6) I	I 108.1 (−2.2) SmC 58.7 (−15.7) Cr
12PB-N	Cr 80.2 (26.1) SmC 111.2 (3.1) I	I 108.9 (−2.9) SmC 64.7 (−25.7) Cr
14PB-N	Cr 89.5 (34.6) SmC 111.4 (3.0) I	I 107.8 (−2.8) SmC 67.4 (−26.7) Cr
16PB-N	Cr 93.1 (39.2) SmC 108.8 (3.0) I	I 106.1 (−3.0) SmC 71.3 (−31.2) Cr
18PB-N	Cr 99.0–100.2 (n.d.) I	I 99.1-97.9 Cr

Cr: crystal; SmC: smectic C mesophase; I: isotropic liquid.

Table 2. Types of phase transitions, temperatures, and corresponding enthalpies obtained by POM and DSC methods for compounds **nPB-M**

	Transition temperature/°C (enthalpy change/kJ mol^{-1})	
Compounds	Heating process	Cooling process
7PB-M	Cr 68.5–69.8 (n.d.) I	I 67.4–66.1 Cr
8PB-M	Cr 72.6 (50.3) SmC 75.7 (8.3) I	I 72.8 (−7.9) SmC 69.5 (−47.2.) Cr
10PB-M	Cr 65.3 (40.2) SmC 80.7 (7.5) I	I 77.7 (−7.5) SmC 41.1 (−33.4) Cr
12PB-M	Cr 69.8 (46.8) SmC 82.3 (9.0) I	I 78.5 (−9.0) SmC 52.4 (−46.0) Cr
14PB-M	Cr 65.3 (33.5) SmC 83.5 (7.9) I	I 80.1 (−6.9) SmC 48.9 (−30.5) Cr
16PB-M	Cr 72.5 (28.3) SmC 81.2 (4.4) I	I 77.2 (−3.9) SmC 57.9 (−7.2) Cr
18PB-M	Cr 99.5–100.7 (n.d.) I	I 99.2–97.8 Cr

Cr: crystal; SmC: smectic C mesophase; I: isotropic liquid.

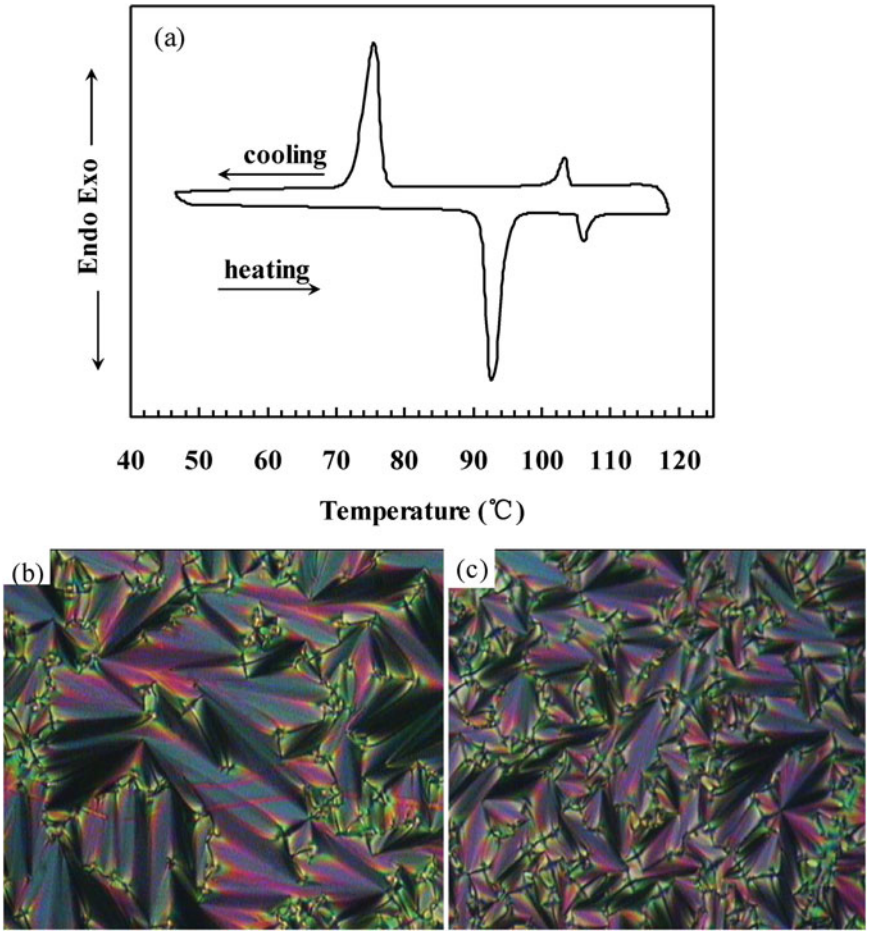

Figure 1. DSC traces and photomicrographs (×200) of **8PB-N**. (a) DSC traces at a scanning rate 5 °C min^{-1}; (b) focal conic textures of the smectic mesophase at 98 °C on heating; and (c) focal conic textures of the smectic mesophase at 80°C on cooling.

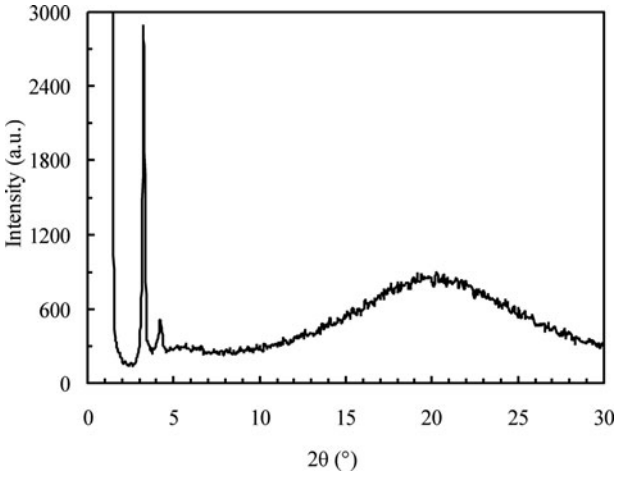

Figure 2. X-ray scattering diagram of **8PB-N** obtained at 98°C on the sample gradually cooled from the isotropic state.

7 °C–32 °C and 12 °C–82 °C for compounds **nPB-C**, respectively, whereas **nPB-H** showed no mesophase at all.

As shown in Table 1, compounds **nPB-N** with a too short or a too long terminal alkoxy chain ($n < 7$ or $n > 16$) exhibited no mesophase at all on heating or cooling, while the other compounds only showed the smectic C mesophase. The phases of **8PB-N** were assigned from the typical fan-shaped textures during both heating and cooling processes, respectively, as shown in Fig. 1. The lamellar structure of this mesophase was also confirmed by the X-ray diffraction (XRD) method. A sharp peak corresponding to an interlayer spacing distance of 2.88 nm in the small angle region and a broad reflection centered near 0.44 nm were observed in XRD diagrams of **8PB-N** at 98 °C (Fig. 2). The calculated dimension of the dimer of **8PB-N** in the longest direction was higher than the experimental interlayer spacing, suggesting its smectic C layer characteristic.

Similar to compounds **nPB-N**, **nPB-M** with proper terminal alkoxy chain ($7 < n < 18$) exhibited smectic C mesophase in heating/cooling processes (Table 2), in which the phases of **12PB-M** were assigned from the typical fan-shaped textures during both heating and cooling processes, respectively, as shown in Fig. 3. 5-Chlorobenzoxazole-terminated compounds **nPB-C** with carbon number of the alkoxy chain from 5 to 18 exhibited enantiotropic smectic mesophase (Table 3), which were assigned from the typical fan-shaped or focal conic textures in heating/cooling processes, as shown in Fig. 4. It is noted that a supercooled phenomena was observed in cooling process for **nPB-N**, **nPB-M**, and **nPB-C** series. This phenomenon is common for calamitic liquid crystalline materials.

Compared with other series, **nPB-H** showed no mesophase at all whether with short or long terminal alkoxy chain during both heating and cooling, which indicated that the substituents (NO_2, CH_3, and Cl) at benzoxazole moiety were helpful to increase the mesophase stability. It is obvious that the substituents with the stronger electron-withdrawing effect let to the wider mesomorphic temperature domain for **nPB-x** due to the stronger dipole–dipole interaction between the molecules, i.e., $NO_2 > Cl > CH_3$, as shown in Tables 1–3 and Fig. 5, which was in accordance with the reference results [16]. It was noted that **nPB-x**

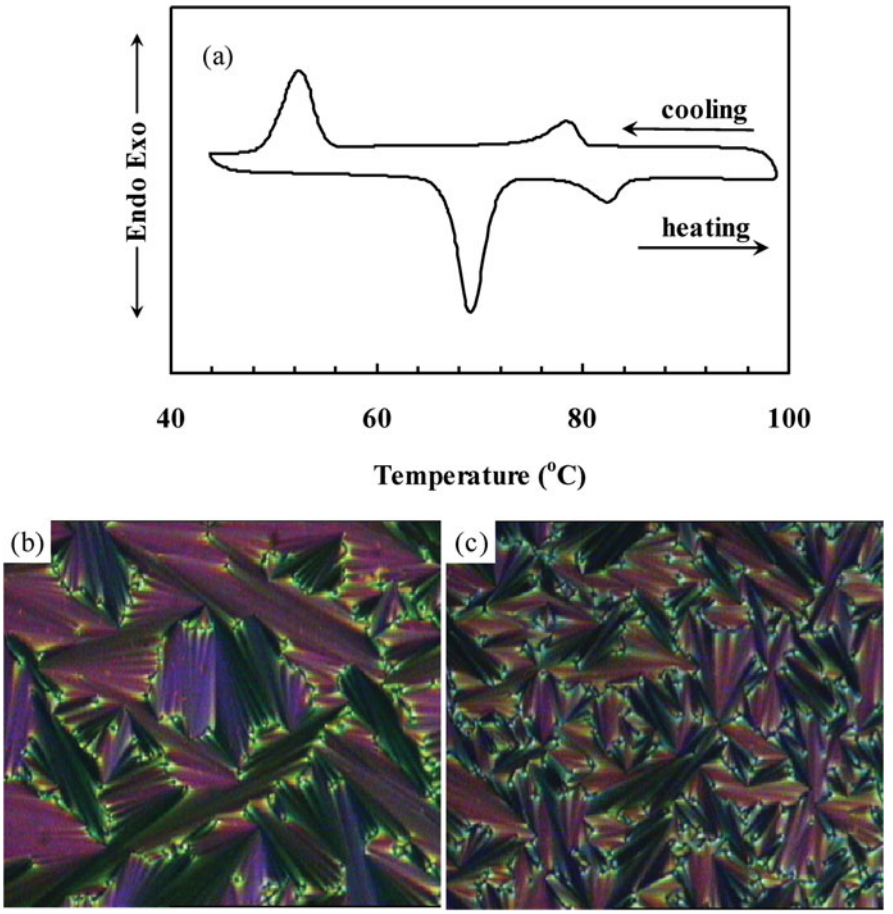

Figure 3. DSC traces and photomicrographs (×200) of **12PB-M**. (a) DSC traces at a scanning rate 5 °C min^{-1}; (b) focal conic textures of the smectic mesophase at 82 °C on heating; and (c) focal conic textures of the smectic mesophase at 70°C on cooling.

exhibited much worse mesophase stability than 2-(4′-alkoxybiphenyl-4-yl)-benzoxazole derivatives, which maybe due to their short mesogenic cores composed of only benzene and substituted benzoxazole.

2.3 Thermal Stability

The thermal stability of **nPB-x** was determined by thermogravimetric analysis (TGA) measurements. Figure 6 depicts the TGA curves of the samples **10PB-N** and **10PB-M**, which were recorded at 30 °C–500 °C under N_2 atmosphere. TGA measurement of compound **10PB-C** was not carried out to avoid the corruption of test cell resulted from chloro. It can be seen that both the compounds **10PB-N** and **10PB-M** were almost completely decomposed by a one-step process from 180 °C to 350 °C, whereas **10PB-N** showed a higher onset decomposition temperature at 245 °C than **10PB-M** (205 °C). This indicated that the decomposition temperature increased with the increase of the polarity of the molecules, where polar nitro substituent in **nPB-N** structure enhanced the dipole–dipole interaction

Table 3. Types of phase transitions and temperatures obtained by POM for compounds **nPB-C**

	Transition temperature/°C	
Compounds	Heating process	Cooling process
3PB-C	Cr 120.1–121.8 I	I 119.3–117.8 Cr
5PB-C	Cr 79.8 SmC 105.6 I	I 103.4 SmC 55.7 Cr
6PB-C	Cr 86.7 SmC 107.8 I	I 104.3 SmC 68.3 Cr
7PB-C	Cr 77.7 SmC 110.1 I	I 107.6 SmC 36.9 Cr
8PB-C	Cr 86.1 SmC 115.3 I	I 112.1 SmC 29.8 Cr
10PB-C	Cr 77.3 SmC 107.8 I	I 104.4 SmC 49.4 Cr
12PB-C	Cr 78.1 SmC 106.9 I	I 102.6 SmC 63.4 Cr
14PB-C	Cr 79.3 SmC 103.4 I	I 101.5 SmC 60.7 Cr
16PB-C	Cr 82.5 SmC 99.6 I	I 96.9 SmC 62.3 Cr
18PB-C	Cr 86.3 SmC 93.1 I	I 90.8 SmC 78.9 Cr

Cr: crystal; SmC: smectic C mesophase; I: isotropic liquid.

between the molecules, resulting in high thermal stability. All the results showed that **nPB-x** series are stable before their clearing point. Those are consistent with the DSC results.

2.4 The Effects of Alkoxy Chain and Polar Substituents on Liquid Crystalline Properties

It is clear that the length of the alkoxy chain influenced not only the nature of the mesophases but also the mesomorphic temperature ranges. Figures 7–9 plot the transition temperatures of compounds **nPB-N**, **nPB-M**, and **nPB-C** as a function of the number of methylenic units (n) in the alkoxy chain during the heating process, respectively.

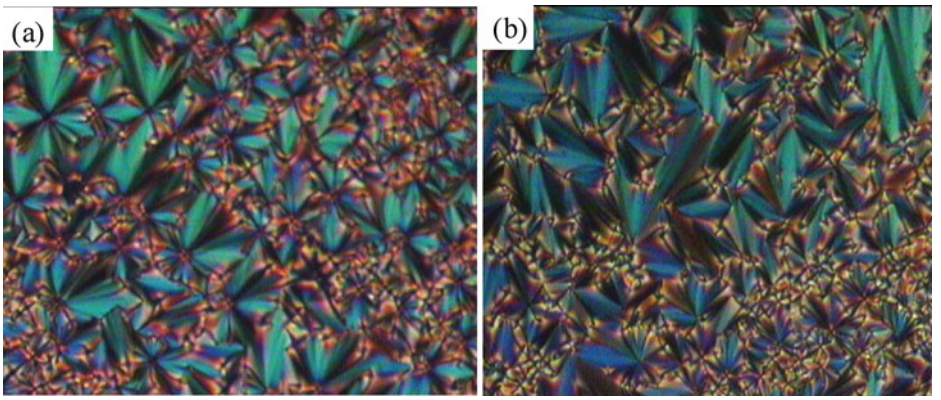

Figure 4. DSC traces and photomicrographs (×200) of **16PB-C**. (a) Focal conic textures of the smectic mesophase at 88°C on heating and (b) focal conic textures of the smectic mesophase at 67 °C on cooling.

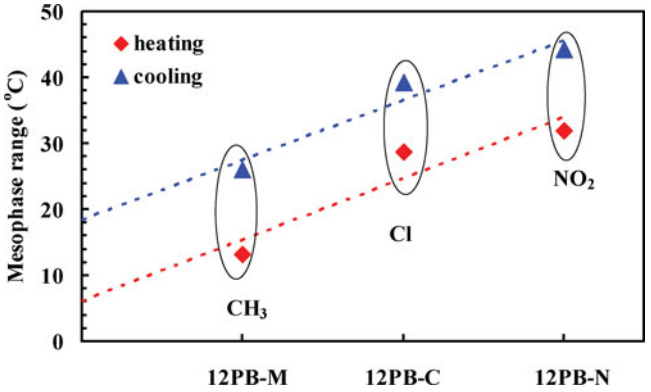

Figure 5. The effect of substituents on the mesophase range of compounds **12PB-X** during heating and cooling.

As shown in Figs. 7–9, a decreasing trend in the melting temperature was observed for the compounds **nPB-N**, **nPB-M**, and **nPB-C** series with alkoxy chain length from 6 to 12 (Fig. 7), 7 to 14 (Fig. 8), and 3 to 10 (Fig. 9), respectively, whereas by ascending the homologs further, an increase in the melting temperature was found. The SmC-isotropic liquid transition temperature increased obviously first, and then decreased smoothly for **nPB-x** with ascending the homologues. As a result, the elongation of the terminal alkoxy chain produced an enhancement of the mesomorphic temperature ranges first, and then followed by a decrease in mesophase range.

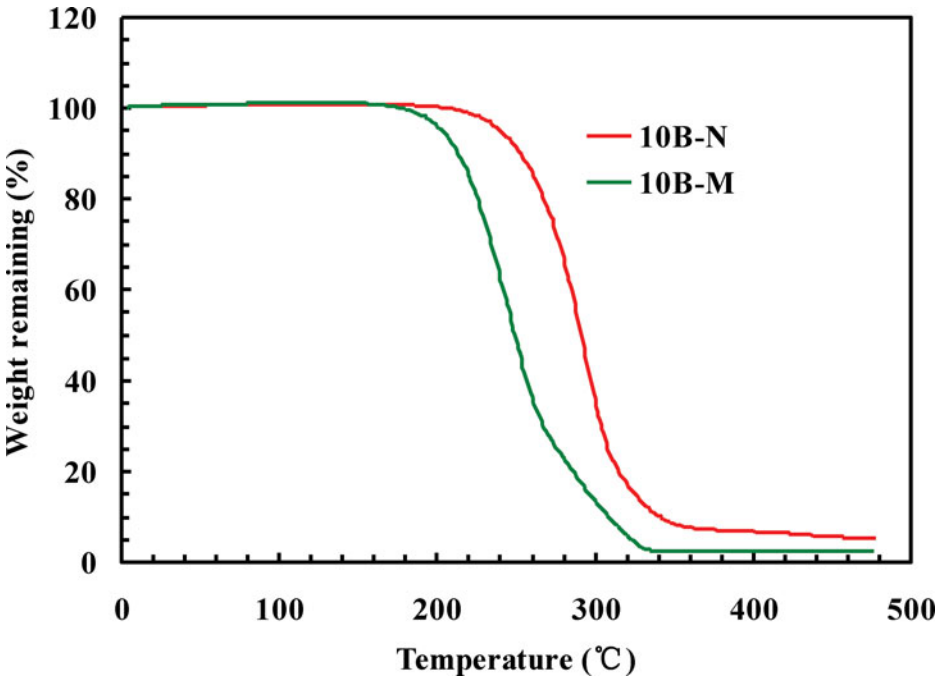

Figure 6. TGA curves of compounds **10PB-x**.

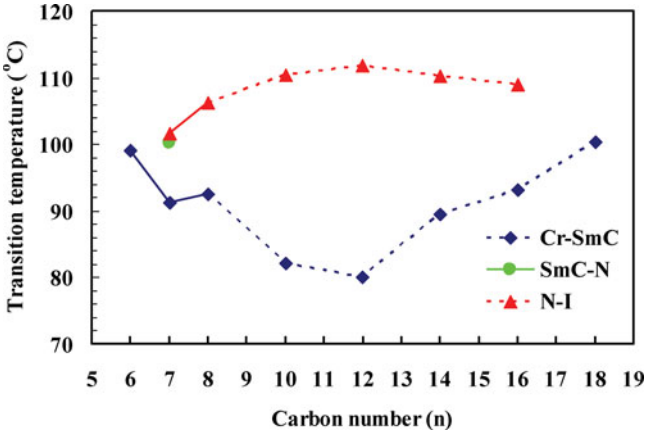

Figure 7. Transition behavior of the compounds **nPB-N** series: dependence of the transition temperatures on the number (n) of methylene units of the alkoxy chain.

Generally, the calamitic compounds substituted with polar groups, such as nitro group, might lead to a higher clearing temperature [15]. In our case, compounds **nPB-x** with electron-withdrawing substituents (x = NO_2, Cl) displayed higher clearing temperatures (T_{cl}) than those of other corresponding homologs with electron-donating substituents, and the higher T_{cl} was attributed to an enhanced conjugative interaction.

2.5 Photophysical Properties

The absorption spectra of compounds **10PB-x** recorded in CH_2Cl_2 are shown in Fig. 10. All of the compounds exhibited a broad absorption band (λ_{max} = 315 nm for **10PB-N**, 315 nm for **10PB-C**, 313 nm for **10PB-M**, and 306 nm for **10PB-H**) attributable to the electronic transition originating from the π-molecular orbitals. Compared with **10PB-H**, the polar substituents at benzoxazole moiety result in a slight redshift of the absorption

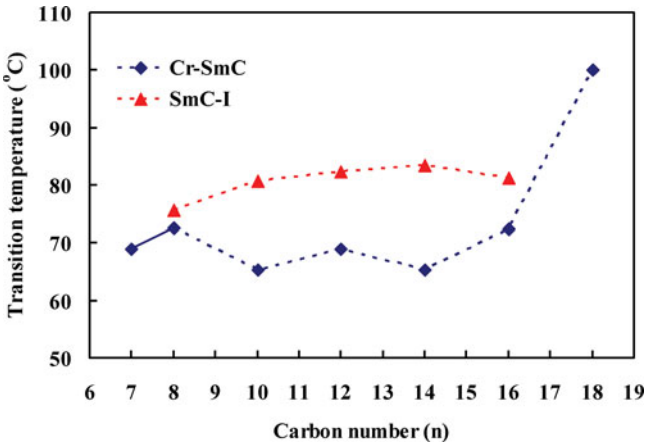

Figure 8. Transition behavior of the compounds **nPB-M** series: dependence of the transition temperatures on the number (n) of methylene units of the alkoxy chain.

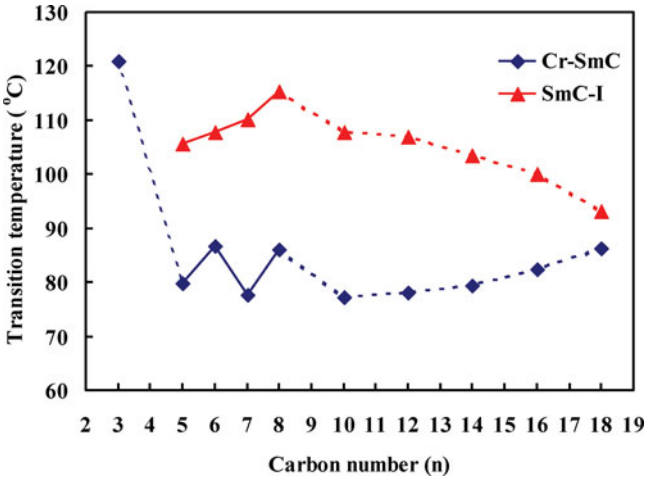

Figure 9. Transition behavior of the compounds **nPB-C** series: dependence of the transition temperatures on the number (*n*) of methylene units of the alkoxy chain.

band in a sequence, which is similar to the effect of the substituents on the mesophase. This phenomenon is related to the strength of π-conjugation resulted from the substituents, for instance, nitro-, chloro-, and methyl-substituted compounds **10PB-N**, **10PB-C**, and **10PB-M** exhibited a slight redshift due to the stronger π–π, p–π, and σ–π conjugation, respectively.

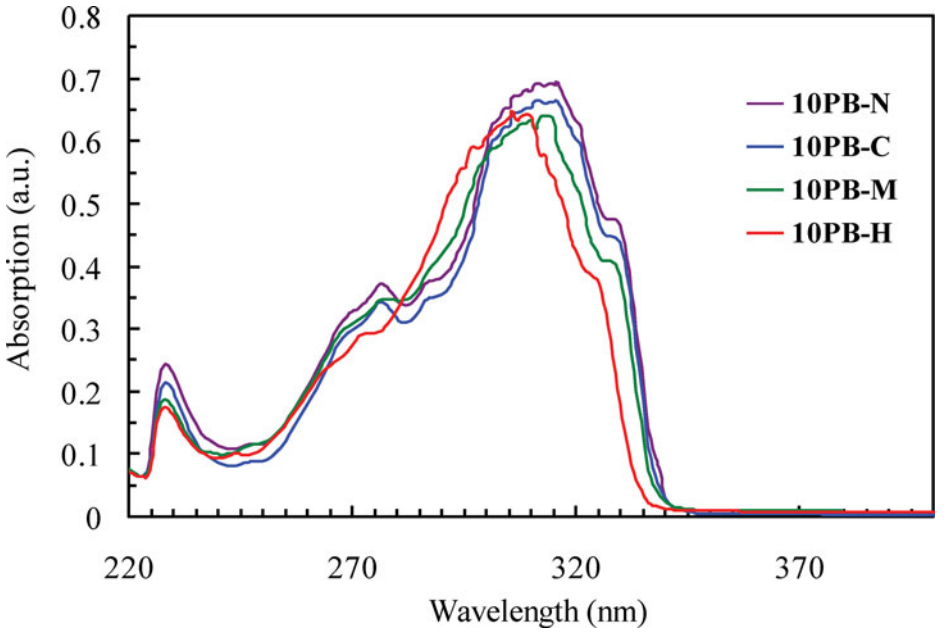

Figure 10. UV spectra of **10PB-x** in CH_2Cl_2 (2.1×10^{-3} mol L^{-1}).

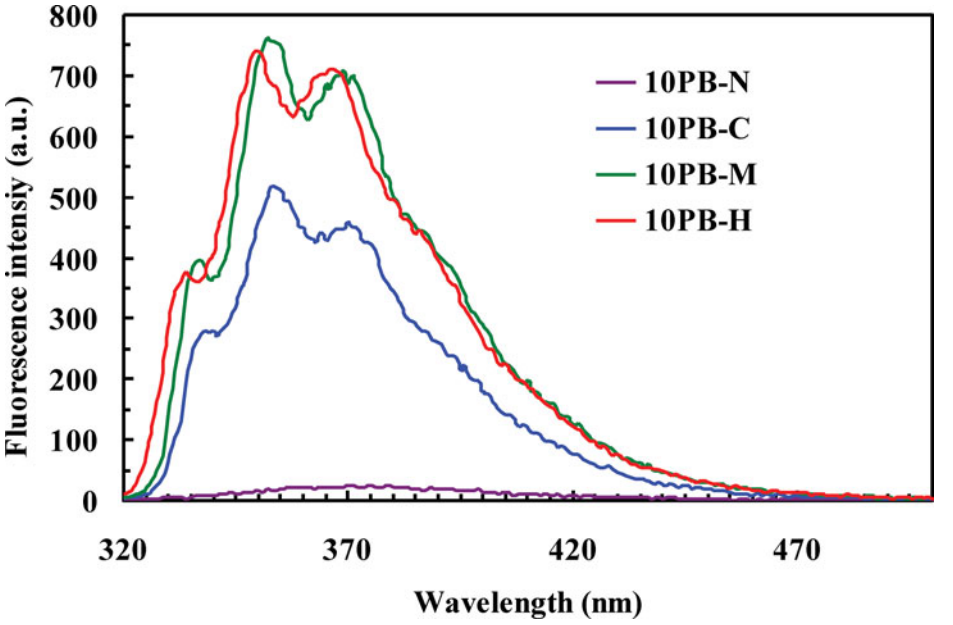

Figure 11. FL spectra of **10PB-x** in CH_2Cl_2 (2.1×10^{-5} mol L^{-1}).

The fluorescence spectra of compounds **10PB-x** were recorded and shown in Fig. 11. The compounds exhibited intense emission in CH_2Cl_2 solutions when excited at their absorption maxima, where the peaks of the emission bands appeared at 350 nm (**10PB-H**), 353 nm (**10PB-M**), and 355 nm (**10PB-C**), respectively, whereas **10PB-N** led to a significant decrease in emission, which was a common phenomenon for nitro-substituted fluorophores. Compared with **10PB-H**, the substituted benzoxazole-terminated compounds showed slight redshifted emission peaks, which was consistent with the trend observed in the absorption spectra.

3. Conclusions

In summary, **nPB-x** bearing different polar substituents (i.e., H, NO_2, CH_3, Cl) at 5-position of benzoxazole moiety were synthesized and characterized. The substituents had obvious effects on the liquid crystal mesophase ranges and the UV absorption bands of **nB-x** with the same sequence. The elongation of the terminal alkoxy chain produced different effects on the melting and clearing points, which resulted in an enhancement of the mesomorphic temperature ranges first, and then followed by a decrease in mesophase range with ascending the homologs. Compared with 2-(4′-alkoxybiphenyl-4-yl) -benzoxazole derivatives, **nPB-x** exhibited much worse mesophase stability due to their short mesogenic cores composed of only benzene and substituted benzoxazole.

4. Experimental

4.1 Materials

4-Hydroxybenzaldehyde, bromoalkanes, 2-amino-4-nitrophenol, 2-amino-4-chlorophenol, 2-amino-4-methylphenol, 2-aminophenol, and DDQ were purchased from Aladdin-Reagent Co. (Shanghai, China) and used as received. Tetrahydrofuran, silica gel, petroleum ether (PE), ethyl acetate (EA), absolute ethanol, N,N-dimethylformamide (DMF), chloroform and anhydrous potassium carbonate were purchased from Sinopharm Chemical Reagent Co. (Shanghai, China) and anhydrous potassium carbonate was dried at 150 °C in vacuum prior to use. Chloroform was dehydrated by pre-dried 4 Å molecular sieves that were activated at 350 °C for 4 hr prior to use.

4.2 Characterization and Measurements

The structures of the final products and intermediates were confirmed by a variety of spectral methods. IR spectra were recorded on a Nicolet Avatar360E spectrometer. ^{1}H-NMR spectra, with tetramethylsilane (TMS) as internal standard, were recorded on a Bruker AV 300 (300 MHz) and AV 400 (400 MHz) instruments. Some of the mass spectra were obtained by GC/EI-MS Thermo DSQ II with *m/z* 50–650. Elemental analysis was performed for C, H, and N in an Elementar Vario EL III instrument. The phase transition temperatures of the target compounds were measured by DSC, Shimatsu DSC-60 in nitrogen at a heating and cooling rate of 5 °C min^{-1}, and POM, Changfang XPN-300E with a heating stage and a control unit. TGA was carried out with a TA 600SDT in helium (flow rate: 100 cm^3 min^{-1}) at a heating rate of 10 °C min^{-1}. UV-vis absorption spectra were recorded using a Hitachi U-3900UV spectrometer. The emission spectra were recorded using a Cary Eclipse spectrometer.

4.3 Synthesis

As an example, the preparation procedure of 2-(4-tetradecyloxyphenyl-1-yl)-5-methyl-benzoxazole (**14PB-M**) is described below.

4.3.1 Synthesis of 4-tetradecyloxybenzaldehyde. To a 50 mL, three-neck, round-bottom flask equipped with an overhead stirrer and condenser, 12.2 g (0.1 mol) of 4-hydroxy benzaldehyde, 30.5 g (0.11 mol) of 1-bromotetradecane, 27.6 g (0.2 mol) of anhydrous potassium carbonate, 0.5 g of KI, and 150 mL of DMF were added. Then the reaction system was stirred at 100 °C for 4 hr. After completion of the reaction, the mixture was diluted with water and filtered. The solid was recrystallized from ethanol.

The yield was 95% of pale white crystals. M.p. 50.6–51.8 °C. ^{1}H-NMR (300 MHz, $CDCl_3$, TMS): δ (ppm) 9.88 (s, 1H), 7.84 (d, $J = 8.7$ Hz, 2H), 7.04 (d, $J = 8.7$ Hz, 2H), 4.04 (t, $J = 6.3$ Hz, 2H), 1.84 (m, 2H), 1.47–1.28 (m, 22H), 0.90 (t, $J = 6.6$ Hz, 3H). IR (KBr, pellet, cm^{-1}): 2918, 2844, 1687, 1595, 1502, 1464, 1379, 1252, 1159, 1028, 827, 719. Elemental analysis: calcd. $C_{21}H_{34}O_2$: C 79.19, H 10.76, N 10.05; found C 80.03, H 10.65, N 9.98.

*4.3.2 Synthesis of 2-(((4-tetradecyloxyphenyl-1-yl)methylene)amino)-4-methylphenol (**14PB-S-M**).* To a 100 mL round-bottom flask equipped with an overhead stirrer and condenser, 1.69 g of 4-tetradecyloxy-benzaldehyde (4.0 mmol), 0.54 g of (4.4 mmol)

2-amino-4-methylphenol, and 40 mL of ethanol were added. The reaction system was stirred at reflux for 6 hr. Then the mixture was cooled to room temperature, it was filtered through Celite. The solid was washed with 15 mL ethanol for several times to give the object with the HPLC purity more than 98%.

The yield was 90% of pale white crystals. M.p. 68.7–69.8 °C. ^{1}H-NMR (300 MHz, $CDCl_3$ TMS): δ (ppm) 8.60 (s, 1H), 7.87 (d, $J = 8.7$ Hz, 1H), 7.08 (s, 1H), 6.99 (m, 3H), 6.91 (d, $J = 8.1$ Hz, 2H), 4.05 (t, $J = 6.3$ Hz, 2H), 2.31 (s, 3H), 1.84 (m, 2H), 1.47–1.28 (m, 22H), 0.90 (t, $J = 6.6$ Hz, 3H). IR (KBr, pellet, cm^{-1}): 3378, 2953, 2916, 2849, 1620, 1603, 1593, 1568, 1514, 1498, 1473, 1451, 1394, 1382, 1337, 1311, 1254, 1248, 1218, 1035, 1023, 1007, 828, 802. Elemental analysis: calcd. $C_{28}H_{41}NO_2$: C 79.39, H 9.76, N 3.31; found C 80.06, H 9.65, N 3.26.

*4.3.3 Synthesis of 2-(tetradecyloxyphenyl-1-yl)-5-methylbenzoxazole (**14PB-M**).* To a 100 mL round-bottom flask equipped with an overhead stirrer and condenser, 0.85 g (2.00 mmol) of **14PB-S-M**, 0.50 g (2.2 mmol) of DDQ, and 50 mL of chloroform were added. The reaction system was stirred at reflux for 6 hr. After completion of the reaction, the mixture was diluted with water and extracted with chloroform for three times. The combined organic phase was dried over $MgSO_4$. After removal of the solvent in vacuo, the residue was purified through recrystallization from ethanol to give the object with the HPLC purity more than 98%.

The yield was 70% of pale white crystals. M.p. 65.3 °C. ^{1}H-NMR (300 MHz, $CDCl_3$, TMS): δ (ppm) 8.18 (d, $J = 8.7$ Hz, 2H), 7.52 (s, 1H), 7.43 (d, $J = 8.4$ Hz, 1H), 7.13 (d, $J = 8.4$ Hz, 1H), 7.02 (d, $J = 8.7$ Hz, 2H), 4.05 (t, $J = 6.6$ Hz, 2H), 2.48 (s, 3H), 1.84 (m, 2H), 1.47–1.28 (m, 22H), 0.90 (t, $J = 6.6$ Hz, 3H). IR (KBr, pellet, cm^{-1}): 3052, 3011, 2936, 2916, 2867, 2849, 1625, 1607, 1583, 1560, 1522, 1560, 1473, 1451, 1417, 1394, 1300, 1275, 1266, 1248, 1167, 1058, 1020, 1009, 924, 865, 809, 759, 735. EI-MS *m/z* (rel. int.): 421.41 (M^+, 15), 225.11 (100), 207.04 (16), 196.19 (5), 73.03 (8). Elemental analysis: calcd. $C_{28}H_{39}NO_2$: C 79.76, H 9.32, N 3.32; found C 80.26, H 9.35, N 3.37.

The other benzoxazole-terminated compounds (**nPB-x)** were prepared according to the similar procedure.

***nPB-M** Series.* **7PB-M**: The yield was 69% of pale white crystals. M.p. 68.5–69.8 °C. ^{1}H-NMR (300 MHz, $CDCl_3$, TMS): δ (ppm) 8.18 (d, $J = 8.4$ Hz, 2H), 7.52 (s, 1H), 7.44 (d, $J = 8.4$ Hz, 1H), 7.14 (d, $J = 8.4$ Hz, 1H), 7.02 (d, $J = 8.4$ Hz, 2H), 4.05 (t, $J = 6.6$ Hz, 2H), 2.48 (s, 3H), 1.84 (m, 2H), 1.47–1.30 (m, 8H), 0.91 (t, $J = 6.6$ Hz, 3H). IR (KBr, pellet, cm^{-1}): 3049, 3017, 2941, 2920, 2863, 2850, 1616, 1605, 1582, 1561, 1532, 1502, 1476, 1466, 1431, 1417, 1390, 1314, 1300, 1275, 1253, 1166, 1052, 1031, 1000, 921, 831, 802, 745. EI-MS *m/z* (rel. int.): 309.18 (M^+, 15.5), 211.07 (100), 183.08 (7), 154.09 (2), 63.05 (3). Elemental analysis: calcd. $C_{21}H_{25}NO_2$: C 77.98, H 7.79, N 4.33; found C 78.43, H 7.96, N 4.21.

8PB-M: The yield was 69% of pale white crystals. M.p. 72.6 °C. ^{1}H-NMR (300 MHz, $CDCl_3$, TMS): δ (ppm) 8.18 (d, $J = 8.7$ Hz, 2H), 7.51 (s, 1H), 7.43 (d, $J = 8.4$ Hz, 1H), 7.13 (d, $J = 8.1$ Hz, 1H), 7.02 (d, $J = 9.0$ Hz, 2H), 4.05 (t, $J = 6.6$ Hz, 2H), 2.48 (s, 3H), 1.84 (m, 2H), 1.47–1.30 (m, 10H), 0.91 (t, $J = 6.6$ Hz, 3H). IR (KBr, pellet, cm^{-1}): 3051, 3018, 2942, 2920, 2865, 2851, 1614, 1607, 1582, 1560, 1531, 1501, 1474, 1467, 1433, 1419, 1391, 1315, 1301, 1277, 1256, 1166, 1074, 1055, 1033, 999, 922, 865, 829, 805, 740. EI-MS *m/z* (rel. int.): 337.30 (M^+, 26), 225.11 (100), 207.05 (4), 196.09 (6), 78.08 (4). Elemental analysis: calcd. $C_{22}H_{27}NO_2$: C 78.30, H 8.06, N 4.15; found C 79.55, H 8.26, N 4.23.

10PB-M: The yield was 68% of pale white crystals. M.p. 65.3 °C. ^{1}H-NMR (300 MHz, $CDCl_3$, TMS): δ (ppm) 8.18 (d, $J = 9.0$ Hz, 2H), 7.52 (s, 1H), 7.43 (d, $J = 8.4$ Hz, 1H), 7.13 (d, $J = 8.1$ Hz, 1H), 7.02 (d, $J = 9.0$ Hz, 2H), 4.05 (t, $J = 6.6$ Hz, 2H), 2.48 (s, 3H), 1.84 (m, 2H), 1.47–1.28 (m, 14H), 0.90 (t, $J = 6.6$ Hz, 3H). IR (KBr, pellet, cm^{-1}): 3063, 2978, 2918, 2865, 2847, 1618, 1606, 1584, 1557, 1502, 1482, 1469, 1466, 1449, 1423, 1384, 1309, 1291, 1271, 1254, 1173, 1130, 1118, 1108, 1058, 1010, 998, 940, 920, 874, 849, 812, 798, 738. EI-MS *m/z* (rel. int.): 365.30 (M^+, 19), 281.09 (24), 225.11 (100), 207.05 (52), 147.07 (4).

12PB-M: The yield was 65% of pale white crystals. M.p. 69.8 °C. ^{1}H-NMR (400 MHz, $CDCl_3$, TMS): δ (ppm) 8.19 (d, $J = 8.8$ Hz, 2H), 7.53 (s, 1H), 7.43 (d, $J = 8.4$ Hz, 1H), 7.13 (d, $J = 8.4$ Hz, 1H), 7.02 (d, $J = 8.8$ Hz, 2H), 4.05 (t, $J = 6.4$ Hz, 2H), 2.48 (s, 3H), 1.84 (m, 2H), 1.47–1.28 (m, 18H), 0.90 (t, $J = 6.4$ Hz, 3H). IR (KBr, pellet, cm^{-1}): 3028, 2943, 2936, 2918, 2866, 2847, 1616, 1606, 1583, 1558, 1500, 1492, 1473, 1465, 1422, 1388, 1308, 1289, 1274, 1250, 1169, 1056, 1032, 1002, 922, 872, 825, 794, 738. EI-MS *m/z* (rel. int.): 393.31 (M^+, 16), 225.12 (100), 207.06 (5), 196.10 (6), 55.06 (4).

16PB-M: The yield was 70% of pale white crystals. M.p. 72.5 °C. ^{1}H-NMR (300 MHz, $CDCl_3$, TMS): δ (ppm) 8.18 (d, $J = 8.7$ Hz, 2H), 7.51 (s, 1H), 7.42 (d, $J = 8.4$ Hz, 1H), 7.13 (d, $J = 8.4$ Hz, 1H), 7.02 (d, $J = 8.7$ Hz, 2H), 4.06 (t, $J = 6.6$ Hz, 2H), 2.48 (s, 3H), 1.84 (m, 2H), 1.47–1.27 (m, 26H), 0.90 (t, $J = 6.6$ Hz, 3H). IR (KBr, pellet, cm^{-1}): 3018, 2941, 2918, 2850, 1604, 1569, 1490, 1473, 1288, 1255, 1062, 1029, 999, 923, 829, 800, 746. EI-MS *m/z* (rel. int.): 449.41 (M^+, 12), 225.12 (100), 207.06 (9), 78.06 (4), 73.05 (4). Elemental analysis: calcd. $C_{30}H_{43}NO_2$: C 80.13, H 9.64, N 3.11; found C 80.68, H 9.71, N 3.10.

18PB-M: The yield was 72% of pale white crystals. M.p. 99.5–100.7 °C. ^{1}H-NMR (300 MHz, $CDCl_3$, TMS): δ (ppm) 8.18 (d, $J = 8.7$ Hz, 2H), 7.51 (s, 1H), 7.42 (d, $J = 8.4$ Hz, 1H), 7.13 (d, $J = 8.4$ Hz, 1H), 7.02 (d, $J = 8.7$ Hz, 2H), 4.06 (t, $J = 6.6$ Hz, 2H), 2.48 (s, 3H), 1.84 (m, 2H), 1.47–1.27 (m, 30H), 0.90 (t, $J = 6.6$ Hz, 3H). IR (KBr, pellet, cm^{-1}): 3051, 3012, 2952, 2939, 2916, 2867, 2847, 1606, 1582, 1554, 1525, 1501, 1471, 1416, 1395, 1303, 1282, 1249, 1168, 1057, 1033, 1004, 924, 830, 808, 718. EI-MS *m/z* (rel. int.): 357 (M^+, 28), 287 (100). Elemental analysis: calcd. $C_{32}H_{47}NO_2$: C 80.45, H 9.92, N 2.93; found C 80.95, H 10.19, N 2.89.

nPB-N Series. **3PB-N**: The yield was 61% of pale white crystals. M.p. 167.8–169.1 °C. ^{1}H-NMR (400 MHz, $CDCl_3$, TMS): δ (ppm) 8.59 (d, $^4J = 2.0$ Hz, 1H), 8.29 (q, $^3J = 8.8$ Hz, $^4J = 2.4$ Hz, 1H), 8.20 (d, $J = 8.8$ Hz, 2H), 7.64 (d, $J = 8.8$ Hz, 1H), 7.05 (d, $J = 8.8$ Hz, 2H), 4.04 (t, $J = 6.4$ Hz, 2H), 1.89 (m, 2H), 1.09 (t, $J = 6.8$ Hz, 3H). IR (KBr, pellet, cm^{-1}): 3123, 3106, 2972, 2937, 2918, 2870, 2850, 1619, 1603, 1578, 1562, 1522, 1500, 1468, 1456, 1428, 1397,1367, 1341, 1309, 1295, 1252, 1231, 1202, 1143, 1117, 1067, 1008, 972, 919, 870, 831, 817, 745. Elemental analysis: calcd. $C_{16}H_{14}N_2O_2$: C 64.42, H 4.73, N 9.39; found C 65.29, H 5.06, N 9.33.

5PB-N: The yield was 60% of pale white crystals. M.p. 161.5–162.3 °C. ^{1}H-NMR (400 MHz, $CDCl_3$, TMS): δ (ppm) 8.59 (d, $^4J = 2.0$ Hz, 1H), 8.29 (q, $^3J = 8.8$ Hz, $^4J = 2.4$ Hz, 1H), 8.20 (d, $J = 8.8$ Hz, 2H), 7.64 (d, $J = 8.8$ Hz, 1H), 7.05 (d, $J = 8.8$ Hz, 2H), 4.06 (t, $J = 6.4$ Hz, 2H), 1.85 (m, 2H), 1.49 (m 4H), 0.97 (t, $J = 6.8$ Hz, 3H). IR (KBr, pellet, cm^{-1}): 3095, 2968, 2929, 2871, 1619, 1600, 1554, 1522, 1493, 1474, 1424, 1340, 1301, 1251, 1186, 1047, 1012, 972, 810, 743. Elemental analysis: calcd. $C_{18}H_{18}N_2O_2$: C 66.25, H 5.56, N 8.58; found C 67.03, H 5.72, N 8.61.

6PB-N: The yield was 62% of pale white crystals. M.p. 99.0–100.2 °C. ^{1}H-NMR (400 MHz, $CDCl_3$, TMS): δ (ppm) 8.58 (d, $^4J = 2.0$ Hz, 1H), 8.28 (q, $^3J = 8.8$ Hz,

^4J = 2.4 Hz, 1H), 8.19 (d, J = 8.8 Hz, 2H), 7.63 (d, J = 8.8 Hz, 1H), 7.04 (d, J = 8.8 Hz, 2H), 4.05 (t, J = 6.4 Hz, 2H), 1.84 (m, 2H), 1.51–1.36 (m 6H), 0.92 (t, J = 6.8 Hz, 3H). IR (KBr, pellet, cm^{-1}): 2949, 2915, 2868, 2840, 1623, 1605, 1560, 1524, 1499, 1460, 1425, 1396, 1382, 1361, 1342, 1305, 1342, 1306, 1293, 1256, 1234, 1170, 1117, 1041, 1001, 839, 823, 810, 743, 733. Elemental analysis: calcd. $C_{19}H_{20}N_2O_2$: C 67.05, H 5.92, N 8.23; found C 67.78, H 6.19, N 8.27.

7PB-N: The yield was 59% of pale white crystals. M.p. 90.9 °C. ^{1}H-NMR (400 MHz, $CDCl_3$, TMS): δ (ppm) 8.60 (d, ^4J = 2.0 Hz, 1H), 8.29 (q, ^3J = 8.8 Hz, ^4J = 2.4 Hz, 1H), 8.20 (d, J = 8.8 Hz, 2H), 7.64 (d, J = 8.8 Hz, 1H), 7.05 (d, J = 8.8 Hz, 2H), 4.07 (t, J = 6.4 Hz, 2H), 1.86 (m, 2H), 1.52–1.32 (m 8H), 0.92 (t, J = 6.8 Hz, 3H). IR (KBr, pellet, cm^{-1}): 3098, 2938, 2916, 2867, 2851, 1611, 1603, 1577, 1550, 1523, 1497, 1464, 1435, 1391, 1343, 1321, 1302, 1251, 1230, 1202, 1168, 1112, 1067, 1033, 1003, 915, 841, 826, 809, 743. Elemental analysis: calcd. $C_{20}H_{22}N_2O_2$: C 67.78, H 6.26, N 7.90; found C 68.77, H 6.70, N 3.94.

8PB-N: The yield was 61% of pale white crystals. M.p. 92.8 °C. ^{1}H-NMR (400 MHz, $CDCl_3$, TMS): δ (ppm) 8.60 (d, ^4J = 2.0 Hz, 1H), 8.30 (q, ^3J = 8.8 Hz, ^4J = 2.4 Hz, 1H), 8.21 (d, J = 8.8 Hz, 2H), 7.65 (d, J = 8.8 Hz, 1H), 7.06 (d, J = 8.8 Hz, 2H), 4.08 (t, J = 6.4 Hz, 2H), 1.86 (m, 2H), 1.49–1.30 (m 10H), 0.90 (t, J = 6.8 Hz, 3H). IR (KBr, pellet, cm^{-1}): 3117, 3078, 2957, 2936, 2917, 2867, 2852, 1615, 1600, 1578, 1553, 1524, 1497, 1467, 1456, 1429, 1425, 1392, 1343, 1304, 1255, 1237, 1166, 1116, 1071, 1042, 1017, 997, 938, 917, 892, 843, 808, 745. Elemental analysis: calcd. $C_{21}H_{24}N_2O_2$: C 68.46, H 6.57, N 7.60; found C 68.72, H 6.70, N 7.59.

10PB-N: The yield was 55% of pale white crystals. M.p. 82.1 °C. ^{1}H-NMR (400 MHz, $CDCl_3$, TMS): δ (ppm) 8.60 (d, ^4J = 2.0 Hz, 1H), 8.30 (q, ^3J = 8.8 Hz, ^4J = 2.4 Hz, 1H), 8.27 (d, J = 8.8 Hz, 2H), 7.65 (d, J = 8.8 Hz, 1H), 7.06 (d, J = 8.8 Hz, 2H), 4.08 (t, J = 6.4 Hz, 2H), 1.86 (m, 2H), 1.49–1.29 (m 14H), 0.89 (t, J = 6.8 Hz, 3H). IR (KBr, pellet, cm^{-1}): 3115, 3080, 2953, 2929, 2915, 2869, 2848, 1615, 1601, 1580, 1550, 1522, 1496, 1468, 1424, 1346, 1310, 1304, 1293, 1251, 1237, 1166, 1105, 1013, 1003, 938, 917, 893, 844, 823, 807, 745. Elemental analysis: calcd. $C_{23}H_{28}N_2O_2$: C 69.67, H 7.12, N 7.07; found C 70.26, H 7.22, N 7.10.

12PB-N: The yield was 61% of pale white crystals. M.p. 80.2 °C. ^{1}H-NMR (400 MHz, $CDCl_3$, TMS): δ (ppm) 8.60 (d, ^4J = 2.0 Hz, 1H), 8.30 (q, ^3J = 8.8 Hz, ^4J = 2.4 Hz, 1H), 8.27 (d, J = 8.8 Hz, 2H), 7.65 (d, J = 8.8 Hz, 1H), 7.06 (d, J = 8.8 Hz, 2H), 4.07 (t, J = 6.4 Hz, 2H), 1.85 (m, 2H), 1.50–1.27 (m 18H), 0.90 (t, J = 6.8 Hz, 3H). IR (KBr, pellet, cm^{-1}): 3097, 3073, 3043, 2955, 2915, 2869, 2847, 1615, 1604, 1577, 1532, 1499, 1471, 1462, 1424, 1380, 1349, 1322, 1285, 1260, 1237, 1169, 1118, 1067, 1045, 1028, 1023, 1001, 973, 944, 840, 830, 811, 745. Elemental analysis: calcd. $C_{25}H_{32}N_2O_2$: C 70.73, H 7.60, N 6.60; found C 69.38, H 7.70, N 6.87.

14PB-N: The yield was 60% of pale white crystals. M.p. 89.5 °C. ^{1}H-NMR (400 MHz, $CDCl_3$, TMS): δ (ppm) 8.60 (d, ^4J = 2.0 Hz, 1H), 8.30 (q, ^3J = 8.8 Hz, ^4J = 2.4 Hz, 1H), 8.27 (d, J = 8.8 Hz, 2H), 7.65 (d, J = 8.8 Hz, 1H), 7.05 (d, J = 8.8 Hz, 2H), 4.08 (t, J = 6.4 Hz, 2H), 1.85 (m, 2H), 1.48–1.26 (m 22H), 0.89 (t, J = 6.4 Hz, 3H). IR (KBr, pellet, cm^{-1}): 3105, 2943, 2930, 2914, 2865, 2847, 1617, 1600, 1535, 1499, 1469, 1435, 1424, 1360, 1342, 1307, 1302, 1250, 1191, 1167, 1100, 1070, 1037, 1023, 1007, 919, 880, 830, 810, 740. Elemental analysis: calcd. $C_{27}H_{36}N_2O_2$: C 71.65, H 8.02, N 6.19; found C 72.51, H 8.04, N 6.10.

16PB-N: The yield was 62% of pale white crystals. M.p. 93.1 °C. ^{1}H-NMR (400 MHz, $CDCl_3$, TMS): δ (ppm) 8.60 (d, ^4J = 2.0 Hz, 1H), 8.29 (q, ^3J = 8.8 Hz, ^4J = 2.4 Hz, 1H), 8.20 (d, J = 8.8 Hz, 2H), 7.64 (d, J = 8.8 Hz, 1H), 7.05 (d, J = 8.8 Hz, 2H), 4.07

(t, $J = 6.4$ Hz, 2H), 1.86 (m, 2H), 1.52–1.26 (m 22H), 0.89 (t, $J = 6.8$ Hz, 3H). IR (KBr, pellet, cm^{-1}): 3095, 2946, 2933, 2915, 2867, 2848, 1617, 1604, 1579, 1552, 1535, 1499, 1471, 1461, 1452, 1436, 1424, 1380, 1347, 1317, 1261, 1238, 1167, 1110, 1067, 1035, 1001, 918, 886, 842, 811, 759, 744. Elemental analysis: calcd. $C_{29}H_{40}N_2O_2$: C 72.47, H 8.39, N 5.83; found C 71.66, H 8.47, N 5.70.

18PB-N: The yield was 61% of pale white crystals. M.p. 99.0–100.2 °C. ^{1}H-NMR (400 MHz, $CDCl_3$, TMS): δ (ppm) 8.60 (d, $^4J = 2.0$ Hz, 1H), 8.30 (q, $^3J = 8.8$ Hz, $^4J = 2.4$ Hz, 1H), 8.21 (d, $J = 8.8$ Hz, 2H), 7.65 (d, $J = 8.8$ Hz, 1H), 7.05 (d, $J = 8.8$ Hz, 2H), 4.07 (t, $J = 6.4$ Hz, 2H), 1.85 (m, 2H), 1.52–1.26 (m 26H), 0.90 (t, $J = 6.4$ Hz, 3H). IR (KBr, pellet, cm^{-1}): 3097, 2953, 2916, 2848, 1616, 1603, 1578, 1560, 1534, 1500, 1471, 1461, 1424, 1347, 1321, 1304, 1279, 1262, 1237, 1169, 1068, 1005, 981, 938, 919, 842, 811, 745, 735, 718, 690, 662, 518. Elemental analysis: calcd. $C_{31}H_{44}N_2O_2$: C 73.19, H 8.72, N 5.51; found C 73.85, H 9.01, N 5.50.

***nPB-C** Series.* **3PB-C**: The yield was 68% of pale pink crystals. M.p. 120.1–121.8 °C .^{1}H-NMR (400 MHz, $CDCl_3$, TMS): δ (ppm) 8.17 (d, $J = 8.8$ Hz, 2H), 7.70 (d, $^4J = 2.0$ Hz, 1H), 7.46 (d, $J = 8.4$ Hz, 1H), 7.29 (q, $^3J = 8.4$ Hz, $^4J = 2.0$ Hz, 1H), 7.02 (d, $J = 8.8$ Hz, 2H), 4.02 (t, $J = 6.8$ Hz, 2H), 1.86 (m, 2H), 1.08 (t, $J = 7.2$ Hz, 3H). IR (KBr, pellet, cm^{-1}): 2963, 2936, 2913, 2870, 1613, 1603, 1577, 1554, 1501, 1458, 1438, 1421, 1381, 1273, 1259, 1246, 1227, 1175, 1060, 1008, 916, 853, 838, 799, 740. EI-MS *m/z* (rel. int.): 287.10 (M^+, 31), 245.04 (100), 216 (7), 182.10 (2), 126.05 (3). Elemental analysis: calcd. $C_{16}H_{14}NClO_2$: C 66.79, H 4.90, N 4.87; found C 67.24, H 5.14, N 4.91.

5PB-C: The yield was 64% of pale pink crystals. M.p. 79.8 °C. ^{1}HNMR (400 MHz, $CDCl_3$, TMS): δ (ppm) 8.17 (d, $J = 8.4$ Hz, 2H), 7.70 (d, $^4J = 2.0$ Hz, 1H), 7.46 (d, $J = 8.4$ Hz, 1H), 7.29 (q, $^3J = 8.4$ Hz, $^4J = 2.0$ Hz, 1H), 7.02 (d, $J = 9.2$ Hz, 2H), 4.05 (t, $J = 6.8$ Hz, 2H), 1.85 (m, 2H), 1.49 (m, 4H), 0.95 (t, $J = 7.2$ Hz, 3H). IR (KBr, pellet, cm^{-1}): 3096, 2953, 2929, 2914, 2871, 2846, 1618, 1597, 1582, 1555, 1502, 1471, 1462, 1448, 1419, 1382, 1291, 1256, 1174, 1066, 1021, 936, 920, 877, 843, 823, 810, 768, 753, 738. EI-MS *m/z* (rel. int.): 315.15 (M^+, 20), 245.03 (100), 216.06 (8), 153.06 (3),126.06 (3). Elemental analysis: calcd. $C_{18}H_{18}NClO_2$: C 68.46, H 5.75, N 4.44; found C 69.80, H 6.05, N 4.68.

6PB-C: The yield was 60% of pale pink crystals. M.p. 86.7 °C. ^{1}H-NMR (400 MHz, $CDCl_3$, TMS): δ (ppm) 8.17 (d, $J = 9.2$ Hz, 2H), 7.70 (d, $^4J = 2.0$ Hz, 1H), 7.47 (d, $J = 8.4$ Hz, 1H), 7.29 (q, $^3J = 8.4$ Hz, $^4J = 2.0$ Hz, 1H), 7.03 (d, $J = 8.8$ Hz, 2H), 4.06 (t, $J = 6.4$ Hz, 2H), 1.84 (m, 2H), 1.50 (m, 4H), 1.39 (m, 4H), 0.94 (t, $J = 7.2$ Hz, 3H). IR (KBr, pellet, cm^{-1}): 3064, 2945, 2938, 2918, 2857, 1612, 1596, 1578, 1554, 1497, 1472, 1451, 1441, 1378, 1292, 1255, 1231, 1168, 1125, 1023, 915, 881, 836, 800, 738. EI-MS *m/z* (rel. int.): 329.16 (M^+, 22), 245.05 (100), 216,06 (9), 153.06 (3), 126.02 (2).

7PB-C: The yield was 62% of pale pink crystals. M.p. 77.7 °C. ^{1}H-NMR (400 MHz, $CDCl_3$, TMS): δ (ppm) 8.17 (d, $J = 9.2$ Hz, 2H), 7.70 (d, $^4J = 2.0$ Hz, 1H), 7.47 (d, $J = 8.4$ Hz, 1H), 7.29 (q, $^3J = 8.4$ Hz, $^4J = 2.0$ Hz, 1H), 7.03 (d, $J = 8.8$ Hz, 2H), 4.06 (t, $J = 6.4$ Hz, 2H), 1.84 (m, 2H), 1.50 (m, 4H), 1.39 (m, 6H), 0.92 (t, $J = 7.2$ Hz, 3H). IR (KBr, pellet, cm^{-1}): 3061, 2938, 2920, 2849, 1625, 1616, 1596, 1577, 1551, 1496, 1468, 1451, 1423, 1391, 1304, 1292, 1276, 1255, 1235, 1193, 1166, 1122, 1013, 915, 881, 835, 809, 798, 738. EI-MS *m/z* (rel. int.): 343.17 (M^+, 18), 245.03 (100), 216.05(9), 153.08 (2), 126.03 (2). Elemental analysis: calcd. $C_{20}H_{22}NClO_2$: C 69.86, H 6.45, N 4.07; found C 71.30, H 6.54, N 4.16.

8PB-C: The yield was 60% of pale pink crystals. M.p. 86.1 °C. ^{1}H-NMR (400 MHz, $CDCl_3$, TMS): δ (ppm) 8.17 (d, $J = 8.8$ Hz, 2H), 7.70 (d, $^4J = 2.0$ Hz, 1H), 7.47

(d, J = 8.4 Hz, 1H), 7.29 (q, ^3J = 8.4 Hz, ^4J = 2.0 Hz, 1H), 7.03 (d, J = 8.8 Hz, 2H), 4.06 (t, J = 6.4 Hz, 2H), 1.84 (m, 2H), 1.49–1.30 (m, 10H), 0.91 (t, J = 7.2 Hz, 3H). IR (KBr, pellet, cm^{-1}): 3064, 2945, 2938, 2915, 2847, 1611, 1596, 1579, 1555, 1497, 1468, 1451, 1421, 1390, 1304, 1290, 1253, 1231, 1198, 1168, 1060, 1020, 914, 880, 836, 810, 798, 738. EI-MS *m/z* (rel. int.): 357.20 (M^+, 15), 245.05 (100), 207.07 (6), 73.05 (2), 71.09 (3).

10PB-C: The yield was 59% of pale pink crystals. M.p. 77.3 °C. ^{1}H-NMR (300 MHz, $CDCl_3$, TMS): δ (ppm) 8.17 (d, J = 8.7 Hz, 2H), 7.70 (d, ^4J = 1.8 Hz, 1H), 7.47 (d, J = 8.1 Hz, 1H), 7.29 (q, ^3J = 8.1 Hz, ^4J = 1.8 Hz, 1H), 7.03 (d, J = 9.0 Hz, 2H), 4.06 (t, J = 6.6 Hz, 2H), 1.84 (m, 2H), 1.48–1.28 (m, 14H), 0.91 (t, J = 6.6 Hz, 3H). IR (KBr, pellet, cm^{-1}): 3065, 2948, 2936, 2917, 2848, 1612, 1596, 1579, 1555, 1497, 1468, 1448, 1422, 1385, 1290, 1253, 1236, 1197, 1167, 1061, 1053, 1015, 915, 884, 837, 810, 799, 750, 737. EI-MS *m/z* (rel. int.): 385.20 (M^+, 14), 245.05 (100), 216.05 (8), 207.04 (13), 73.07 (5).

12PB-C: The yield was 61% of pale pink crystals. M.p. 78.1 °C. ^{1}H-NMR (400 MHz, $CDCl_3$, TMS): δ (ppm) 8.17 (d, J = 8.8 Hz, 2H), 7.70 (d, ^4J = 2.0 Hz, 1H), 7.47 (d, J = 8.4 Hz, 1H), 7.29 (q, ^3J = 8.4 Hz, ^4J = 2.0 Hz, 1H), 7.03 (d, J = 8.8 Hz, 2H), 4.06 (t, J = 6.4 Hz, 2H), 1.84 (m, 2H), 1.50–1.27 (m, 18H), 0.90 (t, J = 7.2 Hz, 3H). IR (KBr, pellet, cm^{-1}): 3064, 3037, 3020, 2916, 2846, 1616, 1597, 1580, 1554, 1535, 1497, 1470, 1451, 1421, 1390, 1378, 1350, 1305, 1288, 1253, 1236, 1197, 1168, 1063, 1052, 1032, 1015, 1002, 919, 915, 885, 837, 810, 799, 750, 738. EI-MS *m/z* (rel. int.): 413.26 (M^+, 16), 245.05 (100), 216.07 (6), 207.07 (6), 73.05 (3).

14PB-C: The yield was 64% of pale pink crystals. M.p. 79.3 °C. ^{1}H-NMR (400 MHz, $CDCl_3$, TMS): δ (ppm) 8.19 (d, J = 8.8 Hz, 2H), 7.72 (d, ^4J = 2.0 Hz, 1H), 7.48 (d, J = 8.4 Hz, 1H), 7.30 (q, ^3J = 8.4 Hz, ^4J = 2.0 Hz, 1H), 7.03 (d, J = 8.8 Hz, 2H), 4.06 (t, J = 6.4 Hz, 2H), 1.84 (m, 2H), 1.49–1.27 (m, 22H), 0.90 (t, J = 6.4 Hz, 3H). IR (KBr, pellet, cm^{-1}): 3091, 2953, 2929, 2916, 2847, 1618, 1596, 1580, 1555, 1524, 1502, 1471, 1462, 1450, 1419, 1387, 1381, 1288, 1255, 1174, 1051, 1021, 1009, 920, 875, 842, 824, 809, 738. EI-MS *m/z* (rel. int.): 441.32 (M^+, 9), 245.03 (100), 216.08 (4), 207.05 (13), 55.04 (7). Elemental analysis: calcd. $C_{27}H_{36}NClO_2$: C 73.36, H 8.21, N 3.17; found C 74.15, H 8.23, N 3.22.

16PB-C: The yield was 65% of pale pink crystals. M.p. 82.5 °C. ^{1}H-NMR (300 MHz, $CDCl_3$, TMS): δ (ppm) 8.17 (d, J = 8.7 Hz, 2H), 7.70 (d, ^4J = 1.8 Hz, 1H), 7.47 (d, J = 8.7 Hz, 1H), 7.29 (q, ^3J = 8.7 Hz, ^4J = 2.4 Hz, 1H), 7.03 (d, J = 8.7 Hz, 2H), 4.06 (t, J = 6.6 Hz, 2H), 1.84 (m, 2H), 1.48–1.26 (m, 26H), 0.90 (t, J = 6.6 Hz, 3H). IR (KBr, pellet, cm^{-1}): 3067, 2950, 2938, 2918, 2850, 1612, 1597, 1578, 1554, 1528, 1497, 1472, 1466, 1451, 1421, 1392, 1379, 1305, 1293, 1255, 1232, 1196, 1168, 1062, 1023, 1005, 916, 881, 835, 811, 799, 750, 739. EI-MS *m/z* (rel. int.): 469.33 (M^+, 9), 281.10 (11), 245.06 (100), 216.04 (4), 72.99 (12). Elemental analysis: calcd. $C_{29}H_{40}NClO_2$: C 74.09, H 8.58, N 2.98; found C 74.72, H 8.83, N 3.00.

18PB-C: The yield was 61% of pale pink crystals. M.p. 86.3 °C. ^{1}H-NMR (400 MHz, $CDCl_3$, TMS): δ (ppm) 8.17 (d, J = 8.8 Hz, 2H), 7.70 (d, ^4J = 2.0 Hz, 1H), 7.46 (d, J = 8.4 Hz, 1H), 7.29 (q, ^3J = 8.8 Hz, ^4J = 2.0 Hz, 1H), 7.02 (d, J = 8.8 Hz, 2H), 4.05 (t, J = 6.4 Hz, 2H), 1.84 (m, 2H), 1.49–1.28 (m, 30H), 0.90 (t, J = 6.8 Hz, 3H). IR (KBr, pellet, cm^{-1}): 3094, 2953, 2915, 2870, 2847, 1617, 1598, 1581, 1558, 1502, 1471, 1462, 1451, 1419, 1391, 1381, 1255, 1228, 1198, 1174, 1159, 1063, 1051, 1032, 1020, 1008, 920, 880, 844, 837, 809, 750, 738, 729, 719, 702, 663, 596, 541, 527, 514. Elemental analysis: calcd. $C_{31}H_{44}NClO_2$: C 74.74, H 8.90, N 2.81; found C 75.61, H 9.03, N 2.93.

nPB-H Series. **7PB-H**: The yield was 73% of pale white crystals. M.p. 70.1–71.2 °C. ^{1}H-NMR (300 MHz, $CDCl_3$, TMS): δ (ppm) 8.19 (d, $J = 8.7$ Hz, 2H), 7.74 (m, 1H), 7.56 (m, 1H), 7.33 (m, 2H), 7.05 (d, $J = 8.7$ Hz, 2H), 4.06 (t, $J = 6.6$ Hz, 2H), 1.86 (m, 2H), 1.47–1.29 (m, 8H), 0.91 (t, $J = 6.6$ Hz, 3H). IR (KBr, pellet, cm^{-1}): 2948, 2939, 2916, 2867, 2847, 1606, 1582, 1554, 1525, 1501, 1471, 1416, 1395, 1303, 1282, 1249, 1168, 1057, 1033, 1009, 924, 830, 800. EI-MS *m/z* (rel. int.): 309.20 (M^+, 26), 211.11 (100), 207.07 (6), 182.09 (7), 64.03 (2).

8PB-H: The yield was 73% of pale white crystals. M.p. 75.3–76.6 °C. ^{1}H-NMR (300 MHz, $CDCl_3$, TMS): δ (ppm) 8.20 (d, $J = 8.7$ Hz, 2H), 7.75 (m, 1H), 7.56 (m, 1H), 7.34 (m, 2H), 7.03 (d, $J = 9.0$ Hz, 2H), 4.06 (t, $J = 6.3$ Hz, 2H), 1.86 (m, 2H), 1.48–1.30 (m, 10H), 0.90 (t, $J = 6.6$ Hz, 3H). IR (KBr, pellet, cm^{-1}): 2949, 2916, 2867, 2847, 1618, 1604, 1580, 1554, 1525, 1500, 1465, 1453, 1416, 1395, 1303, 1264, 1240, 1168, 1054, 1033, 1000, 921, 838, 797, 743. EI-MS *m/z* (rel. int.): 351.27 (M^+, 14), 2 (100).

10PB-H: The yield was 73% of pale white crystals. M.p. 70.6–71.7 °C. ^{1}H-NMR (300 MHz, $CDCl_3$, TMS): δ (ppm) 8.22 (d, $J = 8.7$ Hz, 2H), 7.76 (m, 1H), 7.57 (m, 1H), 7.36 (m, 2H), 7.04 (d, $J = 9.0$ Hz, 2H), 4.07 (t, $J = 6.6$ Hz, 2H), 1.85 (m, 2H), 1.48–1.28 (m, 14H), 0.90 (t, $J = 6.9$ Hz, 3H). IR (KBr, pellet, cm^{-1}): 2945, 2938, 2919, 2863, 2847, 1618, 1603, 1580, 1558, 1499, 1470, 1452,1419, 1395, 1301, 1280, 1252, 1241, 1161, 1050, 1016, 920, 832, 800, 746. EI-MS *m/z* (rel. int.): 357 (M^+, 28), 287 (100).

12PB-H: The yield was 73% of pale white crystals. M.p. 77.4–78.3 °C. ^{1}H-NMR (300 MHz, $CDCl_3$, TMS): δ (ppm) 8.20 (d, $J = 9.0$ Hz, 2H), 7.75 (m, 1H), 7.56 (m, 1H), 7.34 (m, 2H), 7.03 (d, $J = 8.7$ Hz, 2H), 4.07 (t, $J = 6.3$ Hz, 2H), 1.87 (m, 2H), 1.48–1.27 (m, 18H), 0.90 (t, $J = 6.3$ Hz, 3H). IR (KBr, pellet, cm^{-1}): 2939, 2918, 2857, 2848, 1619, 1600, 1578, 1555, 1496, 1471, 1452, 1418, 1395, 1302, 1282, 1244, 1166, 1058, 1031, 1001, 922, 833, 800, 745. EI-MS *m/z* (rel. int.): 357 (M^+, 28), 287 (100).

14PB-H: The yield was 73% of pale white crystals. M.p. 77.4–78.3 °C. ^{1}H-NMR (300 MHz, $CDCl_3$, TMS): δ (ppm) 8.21 (d, $J = 8.7$ Hz, 2H), 7.75 (m, 1H), 7.55 (m, 1H), 7.33 (m, 2H), 7.04 (d, $J = 8.7$ Hz, 2H), 4.07 (t, $J = 6.6$ Hz, 2H), 1.87 (m, 2H), 1.48–1.27 (m, 18H), 0.90 (t, $J = 6.3$ Hz, 3H). IR (KBr, pellet, cm^{-1}): 2940, 2916, 2855, 2847, 1618, 1601, 1572, 1554, 1495, 1470, 1451, 1419, 1398, 1301, 1279, 1256, 1169, 1052, 1030, 1004, 923, 833, 801, 743. EI-MS *m/z* (rel. int.): 357 (M^+, 28), 287 (100).

16PB-H: The yield was 73% of pale white crystals. M.p. 76.5–77.7 °C. ^{1}H-NMR (300 MHz, $CDCl_3$, TMS): δ (ppm) 8.22 (d, $J = 8.7$ Hz, 2H), 7.76 (m, 1H), 7.57 (m, 1H), 7.34 (m, 2H), 7.04 (d, $J = 9.0$ Hz, 2H), 4.06 (t, $J = 6.3$ Hz, 2H), 1.85 (m, 2H), 1.48–1.27 (m, 26H), 0.90 (t, $J = 6.3$ Hz, 3H). IR (KBr, pellet, cm^{-1}): 2954, 2915, 2870, 2847, 1620, 1603, 1585, 1556, 1524, 1502, 1476, 1415, 1399, 1304, 1256, 1171, 1056, 1022, 1000, 921, 840, 808, 741. EI-MS *m/z* (rel. int.): 357 (M^+, 28), 287 (100).

Acknowledgments

The authors would like to thank the National Science Foundation Committee of China (50802058), Program for Changjiang Scholars and Innovative Research Team in University (IRT1070), Specialized Research Fund for the Doctoral Program of Higher Education (20130202120010), Natural Science Foundation of Shaanxi Province (2012JM2002), Key Technologies R&D Program of Shaanxi Province (2012K08-09), and the Fundamental Research Funds for the Central Universities (GK201101003, GK201302036, GK201302037) for financial support of this work.

References

[1] Sung, H. H., & Lin, H. C. (2004). *Liq. Cryst.*, *31*, 831.
[2] Ha, S.-T., Koh, T.-M., Lee, S.-L., Yeap, G.-Y., Lin, H.-C., & Ong, S.-T. (2010). *Liq. Cryst.*, *37*, 547.
[3] Alderete, J., Belmar, J., Parra, M., Zarraga, M., & Zuniga, C. (2008). *Liq. Cryst.*, *35*, 157.
[4] Yeap, G.-Y., Yam, W.-S., Ito, M. M., Takahashi, Y., Nakamura, Y., Mahmood, W. A. K., Boey, P.-L., Hamid, S. A., & Gorecka, E. (2007). *Liq. Cryst.*, *34*, 649.
[5] Li, Y., Chen, X., Chen, P., An, Z., & Li, J. (2010). *Liq. Cryst.*, *37*, 1549.
[6] Chen, P., Li, Y., Chen, X., & An, Z. (2012). *Liq. Cryst.*, *39*, 1393.
[7] Morita, Y., Kawabe, K., Zhang, F., Okamoto, H., Takenaka, S., & Kita, H. (2005). *Chem. Lett.*, *34*, 1650.
[8] Gallardo, H., Conte, G., Tuzimoto, P. A., Behramand, B., Molin, F., Eccher, J., & Bechtold, I. H. (2012). *Liq. Cryst.*, *39*, 1099.
[9] Aldred, M. P., Vlachos, P., Dong, D., Kitney, S. P., Tsoi, W. C., O'Neill, M., & Kelly, S. M. (2005). *Liq. Cryst.*, *32*, 951.
[10] Lai, C. K., Liu, H.-C., Li, F.-J., Cheng, K.-L., & Sheu, H.-S. (2005). *Liq. Cryst.*, *32*, 85.
[11] Majumdar, K. C., Ghosh, T., Rao, D. S. S., & Prasad, S. K. (2011). *Liq. Cryst.*, *38*, 625.
[12] Majumdar, K. C., Ghosh, T., & Shyam, P. K. (2011). *Liq. Cryst.*, *38*, 567.
[13] Wang, H.-C., Wang, Y.-J., Hu, H.-M., Lee, G.-H., & Lai, C. K. (2008). *Tetrahedron*, *64*, 4939.
[14] Chen, C.-J., Wang, I.-W., Sheu, H.-S., Lee, G.-H., & Lai, C. K. (2011). *Tetrahedron*, *67*, 8120.
[15] Wang, C.-S., Wang, I.-W., Cheng, K.-L., & Lai, C. K. (2006). *Tetrahedron*, *62*, 9383.
[16] Xu, Y., Chen, X., Zhao, F., Fan, X., Chen, P., & An, Z. (2013). *Liq. Cryst.*, *40*, 197.
[17] Collings, P. J., & Hird, M. (1998). *Introduction to Liquid Crystals: Chemistry and Physics*, Taylor & Francis Ltd.: UK.